POLITECNICO
MILANO 1863

SCUOLA DI INGEGNERIA INDUSTRIALE
E DELL'INFORMAZIONE

Executive Summary of the Thesis

Numerical Modelling of Laser-Driven Proton Acceleration with Nanostructured Targets and TW-class Lasers

Laurea Magistrale in Nuclear Engineering - Ingegneria Nucleare

Author: Kevin Ambrogioni

Advisor: Prof. Matteo Passoni

Co-advisors: Alessandro Maffini, Marta Galbiati

Academic year: 2022-2023

1. Introduction

The development of lasers providing high-intensity ($\gtrsim 10^{18}$ W/cm^2) electromagnetic fields in controlled shapes in time and space has opened new branches of investigation in the interaction of light with matter. The irradiation of materials with such light sources causes, in fact, plasma formation and particle acceleration. The use of simple analytical models to explore this physical scenario is hindered by its complexity. Therefore, numerical simulations in which the particles composing the plasma move self-consistently with the electromagnetic fields are necessary. The **particle in-cell (PIC) method**[1] is one of the most common approaches thanks to its capability of unveiling the complexity of the physics of the process with a relatively limited computational cost. The interaction of lasers with solid targets is one of the most studied processes. It can give birth to **Target Normal Sheath Acceleration (TNSA)**, a demonstrated mechanism to accelerate low-mass ions which are naturally present on the surface of the targets as hydro-carbon contaminants. Many strategies have been developed over the years to make this process more efficient. Among all, the use of advanced nanostructured targets such as **double-layer targets (DLTs)** is very promising. DLTs exploit a nanostructured low-density (few mg/cm^3) layer deposited on a metallic film to increase laser energy absorption and can be produced at Nanolab (Politecnico di Milano) laboratories. Despite needing more elaborate modelling, such nanostructured targets could be useful in developing compact radiation sources exploiting **TW-class lasers**. Nevertheless, the modelling of such a regime is not straightforward due to the relatively low laser intensity. Target ionisation and morphology can greatly influence the process. The aim of this thesis work is to analyse and optimise the TNSA process in this context, with a focus on the modelling of the nanostructure.

2. Fundamentals

The majority of the analytical models proposed for TNSA neglect the interaction between the laser and the target: the contaminant ion acceleration is described after the laser has interacted with the material and heated up the electrons. The electron heating and consequent expansion are the drivers of the acceleration of the contaminant ions. The hypothesis is justifiable by observing that the inertia of the ions is

at least three orders of magnitude higher than the electron one. Thus, the ion motion just after the interaction is negligible [1]. One of the most used models is the so-called *sheath model*. It is a quasistatic model assuming fixed electrons during the acceleration of ions, an approximation valid for the highest energy ions which are the first to move. The model provides a scaling for the maximum energy of the contaminant protons in the sheath field which is proportional to the electron mean energy usually estimated, in first approximation, by the so-called **corrected ponderomotive scaling** [1]. Such a model estimates the mean electron energy as $T_e \simeq m_e c^2(\sqrt{1+a_0^2/2}-1)$, where $a_0 = e\sqrt{2I}/(m_e\omega c^{\frac{3}{2}})$ is the normalised vector potential, e is the electron charge, c is the light velocity in vacuum and I is the laser peak intensity.

However, the scaling does not apply in the context of DLTs: a specific one is necessary. A proposal to describe the interaction between the laser pulse and the double-layer target can be given under some simplifications [2]. The heating process of the electrons in the metallic layer is still modelled with the corrected ponderomotive scaling. The low-density layer, instead, is modelled as a totally ionised plasma which responds as a thin lens to laser propagation. Low-density plasmas, in fact, allow the propagation of electromagnetic waves, while high-density ones reflect them. The different behaviour is mainly caused by the electrons. The electron density which defines the border between the two regimes is defined as **critical density** $n_c = m_e\omega/(4\pi e^2)$. This threshold depends on the frequency of oscillation ω of the electromagnetic wave and broadens when electron motion is relativistic (i.e. $a_0 > 1$) due to the increase in their inertia. In this sense a plasma which has an electron density in the order of $0.1n_c < n_e < \gamma_0 n_c$ is called near-critical. $\gamma_0 = \sqrt{1+a_0^2/2}$ is the relativistic parameter. In the low-density layer of a DLT, during the propagation of a laser pulse electrons absorb part of its energy and if their motion becomes relativistic the laser pulse gets focused due to non-linear effects. The position at which the pulse is most focused is called self-focusing length l_f. The model for the DLTs predicts the values for the thickness d_{opt}^{nc} and electron density n_{opt}^{nc} which optimise the laser energy absorption:

$$d_{opt}^{nc} = l_f \simeq w_0\Big(\frac{\gamma_0 n_c}{n_e}\Big)^{\frac{1}{2}}, \tag{1}$$

$$n_{opt}^{nc} \simeq 0.91\gamma_0 n_c\Big(\frac{\lambda}{w_0\sqrt{2\ln 2}}\Big)^2\Big(\tau\frac{c}{\lambda}\Big)^{\frac{2}{3}}, \tag{2}$$

where n_e is the electron density of the nearcritical layer, w_0 is the initial laser spot at the start of the near-critical layer and τ is the laser pulse duration at its intensity full width at half maximum (FWHM).

Near-critical layers are usually not homogeneous. Indeed, the density of gases is orders of magnitude lower than the critical density for commonly used lasers, while the opposite happens with solids. The right density can be achieved in nanofoams produced with **Pulsed Laser Deposition (PLD)** at Nanoloab (Politecnico di Milano). Nanofoams are aggregates of particles with a radius of in the order of tens of nanometers. The intrinsic disorder of the nanofoam structure is related to the non-equilibrium nature of its growth process which determines, also, the final nanofoam morphology. PLD foam growth can be modelled with Diffusion-Limited processes. i.e. the formation of clusters in the PLD chamber is characterised by diffusive processes which make the nanoparticles stick together. Two assessed models can be used in describing the formation of such clusters: the **Diffusion-Limited Aggregation (DLA)** model and the **Diffusion-Limited Cluster-Cluster Aggregation (DLCCA)** model. The first supposes that diffusing nanoparticles stick irreversibly to form clusters one at a time. No interaction among the diffusing particles is considered. The second, instead, makes the hypothesis that the diffusing nanoparticles can interact among themselves forming intermediate clusters which eventually aggregate in forming a unique cluster. Different conditions in the deposition of the foam can make one model more effective than the other in describing the PLD foam structure. The foam structure shows properties typical of fractals. The foam mass distribution M is described by a power law with the fractal dimension D_f as exponent ($M \sim R_g^{D_f}$ with R_g as a characteristic length). D_f is related to the physics of aggregation of the clusters. The characteristic length related to such scaling laws is the so-called gyration radius R_g. It is defined

as the radial distance from the centre at which the total mass of an aggregate should be concentrated to have the same moment of inertia as the real aggregate. The gyration radius is proportional to the number of nanoparticles in the aggregate N and to the radius of the nanoparticles r_{np}. Under the hypothesis that the description of the foam can be performed using its mean gyration radius, the following relation for its density ρ_f can be obtained:

$$\rho_f = k\rho_{np}\left(\frac{r_{np}}{R_g}\right)^{3-D_f}, \tag{3}$$

where $R_g = r_{np}N^{\frac{1}{D_f}}$, ρ_{np} is the density of a single nanoparticle and k is a prefactor containing all the physics behind the aggregation and which is usually below the unitary value. The nanostructure of the near-critical layer, particularly when the laser intensity is relatively low, can greatly affect the interaction between the laser and the target. The effects of the nanostructure can be partially explained in terms of the Coulomb explosion[1] of the nanoparticles composing the foam.
To capture all the physics put in by the nanostructure and the relativistic effects induced by high-intensity lasers, kinetic models [3] are necessary. The analytical solution of such models is not feasible in general cases. The numerical approach is then necessary and the **PIC** [1] is one of the most assessed ones. The PIC is a particle method which approximately solves the collisionless kinetic relativistic model. The particles contained in a plasma are sampled with a lower number of numerical particles having an arbitrarily chosen space extension and a unique velocity. The numerical particles move across a space grid under the effects of the electromagnetic field following the solution of Newton-like relativistic equations. The particles deposit charge and current densities, which are then used to solve the Maxwell system of equations. Also, the ionisation effects can be accounted for by inserting a **Monte Carlo module** in between the calculation of the electromagnetic field and the particle motion. Ionisation can happen due to multiple effects. The tunnel ionisation, i.e. the ionisation happening in the presence of a strong electric field which distorts the atomic potential, is one of the most probable and its ionisation rate can be described by means of the **ADK theory** [4].

3. Objectives and Methods

The **goal of the thesis work** can be articulated into two main points. First of all, assessing a method which allows for the construction of numerical foams having desired density and thickness. Secondly, determining the best set-up characteristics for simulations on the interaction of a class-TW laser with solid targets and demonstrating the feasibility of laser-driven proton sources with such lasers by optimising the coupling between the laser and the target. The first goal was pursued by using a proprietary C++ code which is able to simulate both DLA and DLCCA foams and which is independent on the nanoparticle diameter and density. The other goals were pursued by using two different highly parallelised PIC codes: WarpX, which runs also on GPU-accelerated systems, and Smilei, which allows for the initialisation of whatever complex shape for the plasma. The simulations related to the proprietary code were performed on a personal computer, the ones related to the PIC codes were performed on two different clusters belonging to CINECA (Bologna): the Marconi100 GPU-accelerated cluster to perform simulations in WarpX and the Galileo100 cluster to perform simulations in Smilei.

4. Analysis of the results

Numerical foams having different characteristics were simulated. The main parameter influencing the foam density is N, thus foams having 1, 2, 5, 10, 20, 50, 100, 200, 500, 1000 and 2000 particles per cluster were produced. The formed DLCCA clusters then were deposited on a plane substrate in two different ways: a ballistic deposition and a downward diffusive deposition. The substrate transversal dimension D was set to 500 diameters of nanoparticle. The simulation was performed in a box having the substrate as a base, and a height-to-substrate dimension ratio D_z/D of 2. The clusters were initialised in the deposition randomly on the top of the foam and led to falling. Periodic boundary conditions were applied in the transversal directions. A high number of clusters was deposited and various shots of the deposition process were saved as output files. In figure (1) two shots of

the performed cases are presented.

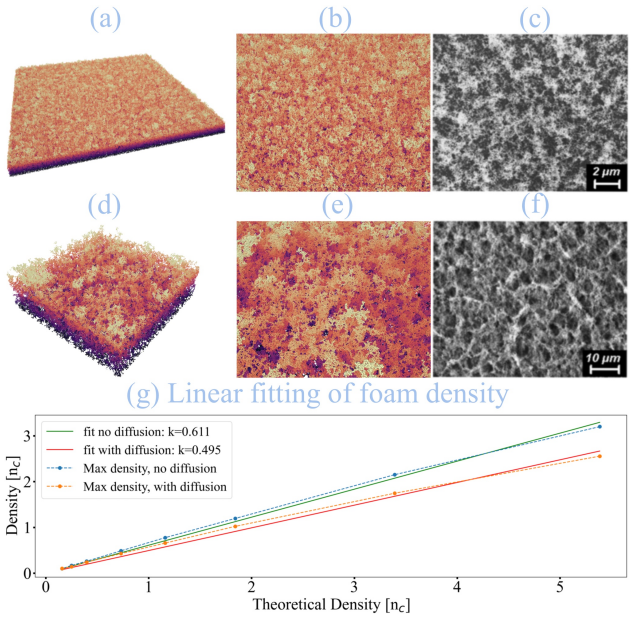

Figure 1: In (a)-(d) the 3D representation of numerical foams ($N = 1$ and $N = 10$), in (b)-(e) the 2D front section of the respective foams, in (c)-(f) a scanning electron microscope (SEM) front section of a DLA and a DLCCA foam (source [5]). Lighter colours are associated with a higher distance from the substrate. In (g) the plot of the estimated density with respect to the theoretical one (equation (3) with $D_f = 1.8$, $\rho_{np} = 25$ n_c, $d_{np} = 25.0$ nm). The dotted line represents the saturated values from the simulations, the continuous line the performed fitting.

In figure (1)-(a) and (b) the representations performed with Ovito of a foam produced with $N = 1$ are shown and compared with a real DLA foam in figure (1)-(c). In figure (1)-(d) and (e) representations of a foam produced with $N = 100$ are shown and compared with a real DLCCA foam in figure (1)-(f). A good accordance between the simulated and real images is observed. Ad-hoc Python tools have been developed to estimate foam density and thickness mimicking experimental methods. Performing a fitting between the theoretical density (formula(3) with $D_f = 1.8$) and the estimated values, two k are retrieved: 0.613 for the ballistic deposition and 0.493 for the diffusive deposition. Then a PIC investigation of the interaction of a **20 TW laser** having a wavelength of 0.8 µm an intensity FWHM of 30 fs and a laser spot of 2.4 µm with a DLT composed of a carbon foam and an aluminium substrate was performed. A first investigation on the effects of the tunnel ionisation process in such a condition was performed with 2D WarpX simulations of a plain substrate, i.e. the worst condition. The results showed that the process could be neglected without losing generality. A parametric scan with 2D simulations was then performed with WarpX analysing different target conditions. The foam density was computed using the relation (2). The substrate density was the realistic aluminium density. Three different substrate (200 nm, 600 nm and 2000 nm) and foam (2 µm, 4 µm, retrieved by the formula (1), and 8 µm) thicknesses were analysed. A hydrogen contaminant layer was positioned on the rear face of the substrate. The results showed that the optimal case (i.e. the case that maximises the proton mean energy and the laser energy conversion into their kinetic energy) in accelerating protons was the 4-µm-thick foam and 200 nm-thick-substrate, in accordance with the analytical model [2]. These results were simulated in two 3D simulations to analyse the effects of the nanostructure. A homogeneous case was simulated with WarpX and a nanostructured case with Smilei. The nanostructure was composed of nanoparticles with a diameter of 80.0 nm and a density of 20.80 n_c. The substrate in both cases was simulated with a reduced electron density of 80 n_c to avoid prohibitive computational costs. The result showed a decrease of the maximum proton energy in the nanostructured case accompanied, however, by an increase in the efficiency in converting laser energy into proton energy (η_p). In figure (2) two shots of the simulation of the nanostructured case are shown (a-b) together with the proton spectrum retrieved at the end of the simulation(c).
Lastly, a PIC investigation of the interaction between a **sub-TW laser** and DLTs was performed. The simulated laser had a pulse energy of 4.5 mJ and a wavelength of 0.8 um. It was modelled in two different conditions: intensity FWHM of 40 fs and laser spot of 3.0 µm and intensity FWHM of 40 fs and laser spot of 2.5 µm. The first part of the investigation was performed by means of 2D simulations. An analysis of the field ionisation process and of the optimal conditions for TNSA were performed in both laser configurations using WarpX. The substrate was

modelled as a 1 µm-thick-aluminium foil with a contaminant layer on the rear surface.

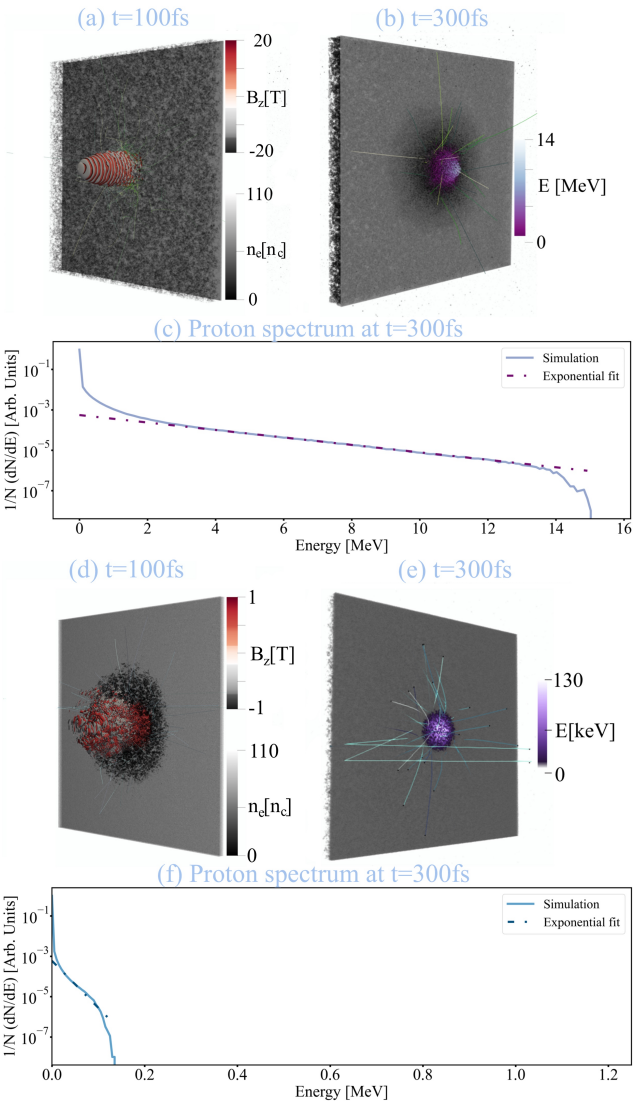

Figure 2: In (a) and (b) the electron density n_e and some electron trajectories in green at two time-steps in the nanostructured 3D 20 TW case. In (a) also the B_z contour and in (b) also the positions of the protons, coloured according to their energy E. In (c) the plot of the proton spectrum at the last time-step, together with the exponential fitting in dotted line. In (d), (e) and (f) the respective for the sub-TW 10 fs FWHM case with a nanostructured foam.

Three different foam conditions were simulated for both the laser configurations with thicknesses retrieved by equation (1). For the 40 fs FWHM case, a 0.3 n_c, calculated from equation (2), a 0.95 n_c, the minimum experimentally achievable density in PLD foams, and a 3 n_c were simulated, while for the 10 fs FWHM case, a 0.2 n_c, calculated from equation (2), a 0.95 n_c and a 3.0 n_c. The results show that ionisation had a great influence on the interaction. The optimal condition for proton acceleration (optimal case) was observed for the 10 fs FWHM laser with the 0.95 n_c foam. Also, simulations neglecting the ionisation process with nanostructured foams were performed with WarpX in both laser conditions and in Smilei for the optimal case analysing the ionisation. The foams in WarpX were modelled taking a slice of a 4 µm DLCCA foam with nanoparticles diameter of 80.0 nm and average densities of 0.95 n_c and 3.0 n_c, the one in Smilei as a slice of a foam obtained from the DLCCA code with clusters having 50 nanoparticles each, with diameter of 50.0 nm. The nanostructure was detrimental both in η_p and in maximum proton energy in the 0.95 n_c cases. The opposite happens in the 3.0 n_c ones. In all cases, an enhanced conversion efficiency of laser energy into foam ion energy (η_f) was observed. An increased mean level of ionisation is also shown with respect to the corresponding homogeneous case in Smilei. Lastly, a 3D nanostructured simulation of the optimal case was performed in Smilei. The foam was modelled as a neutral carbon DLCCA nanostructure with nanoparticles diameter of 50.0 nm and ion density of 4.17 n_c. The substrate was modelled as a three-times-ionised aluminium substrate with a reduced ion density of 6.15 n_c. The result showed a reduced maximum proton energy and η_p. A confirmation of the enhanced η_f was observed. In figure (2) two shots of the simulation of the nanostructured case are shown (d-e) together with the proton spectrum retrieved at the end of the simulation (f).

5. Discussion on the Results

Concerning the **characterisation of the foams** retrieved from the DLCCA code, it is possible to make two main important observations. Firstly, the fitting in figure (1)-(g) was generated by accounting for foams with N up to 10 only. When N is lower than 10 the fitting does not work anymore. The retrieved values for k are in agreement with the experimental ones [5] and with considerations which can be done on the deposition process: k is higher in the ballistic deposition which creates denser aggregates than the diffusion processes. Concerning the **20 TW laser-driven proton ac-**

celeration, a great influence of the substrate thickness in enhancing the TNSA process has been shown. Its influence seems more prominent in the single-layer target where other mechanisms (such as Coulomb explosion of the thin substrate) can play a role in the acceleration in thin targets. The validity of equations (2) and (1) has been demonstrated for this case. The nanostructure presence greatly influences the results: the rising part of the laser pulse does not homogenise the target. A decrease in resonance effects typical of homogeneous near-critical layers can explicate the decrease of proton maximum energy. In the meantime, the Coulomb explosion of foam nanoparticles can be the cause of the increase in η_p. Concerning the **sub-TW laser-driven proton acceleration**, firstly, it was possible to observe that the 10 fs FWHM configuration shows higher proton energy than the 40 fs one. This effect is mainly caused by the overcoming of the relativistic limit for electron motion in such configuration. Secondly, the effect of the foam nanostructure is beneficial in slightly overdense cases because of the propagation of the laser pulse across its void spaces. Moreover, the Coulomb expansion of the foam nanoparticles is at the base, also, of a high η_f. Lastly, the field ionisation effect is fundamental in the PIC modelling of TNSA with sub-TW lasers since the rising part of the pulse is not able to ionise completely the target. The simple model for DLTs[2] fails in estimating the optimal condition in this case, probably as a consequence of neglecting the ionisation process.

6. Conclusions and future developments

This thesis work was carried out with the purpose of modelling numerically the interaction of class-TW lasers with DLTs to demonstrate the feasibility of proton radiation sources using TNSA process. During the thesis work, it was possible to assess the production of numerical DLCCA nanostructures emulating the realistic foams obtained via PLD. This opened the possibility to model numerically the foams which are experimentally produced at Nanolab (Politecnico di Milano). A vast 2D and 3D PIC simulation campaign was then performed to investigate the interaction of a 20 TW and a sub-TW laser with DLTs. In both cases, the definition of optimal set-up conditions for PIC simulations was investigated. The 20 TW laser is not greatly affected by the ionisation process, which can be neglected. On the contrary, such a process must be considered in the sub-TW laser case. Both cases show great dependence on the inclusion of the nanostructure in the numerical modelling. The 20 TW laser, with a maximum proton energy of around 15 MeV and a mean one of around 3 MeV, could be exploited in applications which involve laser-driven PIXE. On the contrary, the low proton mean energy (around tens of keV) makes the sub-TW lasers unapt to perform such analysis. In conclusion, both the laser configuration showed interesting features which must be further investigated. The characterisation of the foams having a number of particles per cluster lower than 10 should be performed and the investigation of other effects in PIC, such as collisions, is necessary. To possibly use TW-class lasers as radiation sources, an improvement of the sub-TW configuration should be investigated and experimental campaigns should be performed, also to confirm the simulation results.

References

[1] A. Macchi. *A Superintense Laser-Plasma Interaction Primer*. Springer Dordrecht, 2013.

[2] A. Pazzaglia et al. A theoretical model of laser-driven ion acceleration from near-critical double-layer targets. *Comm. Phys.*, 3:133, 2020.

[3] Y. L. Klimontovich. *The Statistical Theory of Non-Equilibrium Processes in a Plasma*. Pergamon, 1967.

[4] M. V. Ammosov et al. Tunnel ionization of complex atoms and of atomic ions in an alternating electromagnetic field. *Zhurnal Eksperimental'noi i Teoreticheskoi Fiziki*, 91(6):2008–2013, 1986.

[5] A. Maffini et al. Pulsed laser deposition of carbon nanofoam. *Applied Surface Science*, 599:153859, 2022.